81-0208

NASA-TM-81657 19810007538

NASA Technical Memorandum 81657

Mean Rotor Wake Characteristics of an Aerodynamically Loaded 0.5 m Diameter Fan

L. M. Shaw and F. W. Glaser
Lewis Research Center
Cleveland, Ohio

Prepared for the
Nineteenth Aerospace Sciences Meeting
sponsored by the American Institute of
Aeronautics and Astronautics
St. Louis, Missouri, January 12–15, 1981

NASA

MEAN ROTOR WAKE CHARACTERISTICS OF AN AERODYNAMICALLY LOADED 0.5 M DIAMETER FAN

by L. M. Shaw and F. W. Glaser
National Aeronautics and Space Administration
Lewis Research Center
Cleveland, Ohio

SUMMARY

Mean rotor wake properties at several downstream distances behind the rotor of a loaded 1.2 pressure ratio fan were measured with a cross film anemometer in an anechoic wind tunnel. Mean wake characteristics in the midspan and near tip region were determined utilizing an ensemble averaging technique. The upwash and streamwise components of the velocity behind the rotor indicate a complex structure superimposed on the major velocity defects at a downstream spacing of 0.5 rotor chords. Spectral analysis indicates high levels of the second and fourth harmonics of the blade passage frequency in the midspan region while the blade passage frequency and its second and third harmonic are predominant in the tip region.

E-674

INTRODUCTION

One of the major sources of fan noise is thought to be the interaction of rotor wakes with stator vanes. The noise arises from the fluctuating lift force generated on the stators as they encounter the wake field of the rotor blades. The main wake defect causes tone noise at the blade passing frequency and its harmonics while the wake turbulence causes broadband noise. In the tip region of the blades, still another feature of the rotor exit flow that may cause noise are the tip vortices.[1*]. In order to assess the contribution of these rotor wake features to noise and to provide input for sound generation theoretical models, the characteristics of the rotor wakes must be determined as functions of the spatial coordinates and the fan design and operating conditions. The parameters usually prescribed are the magnitude of the wake defect and its width.

Several investigators have experimentally studied wakes behind a compressor rotor using hot-wire anemometry. Hirsch and Kool[2] utilized a single rotating wire to measure the three-dimensional flow field behind the rotor of an axial compressor. Stationary dual wire probes were used by Evans[3] to measure the free-stream turbulence level and the unsteadiness due to periodic fluctuations in both the mean velocity and the air angle at the inlet to a compressor stator vane. Magliozzi[4] utilized a dual probe to measure rotor wake details at the leading edge of a stator assembly on an outdoor test stand. Bennett[5] determined the mean properties of rotor wakes with a three component wire sensor. The triple wire sensor has been greatly utilized by Lakshminarayana and his associates at Pennsylvania State University. Together with Reynolds[6], Lakshminarayana studied lightly loaded rotor wakes with both stationary and rotating sensors. Effects of blade loading were

*Raised numbers refer to references.

studied by varying the incidence angle to the rotor blades. Later with Ravindranath[7], Lakshminarayana extended his measurements of the near wake to the case of a moderately loaded fan.

The present experimental program was part of a larger fan noise program in which fan noise charcteristics were determined as a function of rotor-stator spacing, rotor and stator blade number, and with and without the effects of forward velocity. The present paper studies the effects of downstream distance and forward velocity on the mean rotor wake properties of a loaded 0.5 m fan. The experiments were conducted in the NASA Lewis 9x15-foot low-speed anechoic wind tunnel. The fan stage studied had 15 rotor blades, a design pressure ratio of about 1.2 at a tip speed of 213 m/sec (700 ft/sec). Wake characteristics were measured with a cross film anemometer oriented to sense the streamwise and upwash components of the rotor wakes. The wakes were measured at downstream distances of 0.54, 1.23, and 1.77 rotor chords. The measurements were made at midspan and tip regions of the blades. The data were analyzed to yield the magnitude and width of the wake defect which are the descriptors usually employed when in the reference frame of the rotor. Comparison of these measured descriptors with those reported in literature was not made, however, because few researchers have reported these descriptors of rotor wakes in the stator reference frame. Finally, an approach offering a more detailed way of describing wake structure is also examined. This approach involved the Fast Fourier Transform of the signal enhanced wake waveform to yield the amplitude of the spatial harmonics of the wakes. In this form the data should be useful in models of fan noise generation.

APPARATUS AND PROCEDURE

Experimental Test Facility

The NASA Lewis 9x15 anechoic wind tunnel is located in the return loop of the 8x6 supersonic tunnel. The aerodynamic and acoustic properties of the low-speed section are documented in references 8 and 9. The airflow in the test section is varied by control of both the tunnel drive motor speed and the position of the control doors immediately upstream of the test section. The tunnel was operated both statically and with a velocity of 41 m/sec.

Fan and Installation

The 50.8-cm diameter fan has 15 blades and 25 vanes. The vanes were positioned at three different mean rotor blade chord spacings: 0.54 chord; 1.23 chord; and 1.77 chord. The spacings were based on a 7.7 cm midspan aerodynamic rotor chord. For the results presented here, the fan was run at 96 percent of the design speed of 8020 rpm corresponding to a tip speed of 197 m/sec. The fan design pressure ratio and work coefficient (change in tangential velocity normalized by tip speed) were 1.16 and 0.42, respectively. Based on the work coefficient, the present fan has a slightly higher loading than the fan tested by Ravindranath and Lakshminarayana.[7] The aerodynamic performance of the fan is documented in reference 10.

A conventional low throat Mach number (0.60) flight inlet was used for the tests. The 1.46 contraction ratio inlet had a 2:1 elliptically contoured lip and a length of approximately 52.6 cm. Aerodynamic performance of the inlet can be found in reference 11. The installation of the fan in

the wind tunnel is seen in figure 1. Shown in the photo is a rotating microphone boom along with several aft microphones. The acoustic data from these microphones are not presented in this paper.

Instrumentation and Procedure

Rotor wake properties were measured with a cross film anemometer. Each film was 70 μm in diameter and 1.25 mm long. The cross film anemometer was located in the plane of the leading edge of the stator vanes midway between two vanes (fig. 2) except for one series of experiments. In that series, the anemometer was located midway between two vanes but upstream of the stator leading edge plane. Since the measurements were all midway between vanes even when in the plane of the stator leading edge, any effect due to the proximity of the stators was expected to be small.

The following table lists the axial spacings of the anemometer and stator vanes from the rotor blades for each test condition.

Test Series	Rotor-stator spacing (rotor chords)	Rotor-anemometer spacing (rotor chords)
1	0.54	0.54
2	1.77	1.23
3	1.77	1.77

Measurements were made at several radial positions. Data near the blade tip (1.27 cm immersion) and the midspan region (7.21 cm immersion) are presented in this paper. The anemometer signals were linearized, summed and differenced and d.c. suppressed before being recorded on magnetic tape. Analysis of the data was done off-line utilizing a digital signal processor.

Figure 3 shows schematically the film orientation and the fluctuating velocity across a wake behind a rotor blade as it appears to a stator vane. The following table lists typical values of the streamwise Mach number measured by the cross film probe and probe set angles at 96 percent of design speed.

	Streamwise Mach number	Probe set angle
Tip region	0.43	28.9°
Midspan region	.49	32.7°

The streamwise velocity changes magnitude as it fluctuates between the angles $\beta \pm \theta$. The cross film was oriented so that the mean streamwise velocity component into the stator would bisect the angles formed by the two films. The cross film had been calibrated for yaw angle before the test so that the fluctuating angle (θ) would be measured accurately. The orientation of the cross film was such that both the streamwise and upwash components of the flow entering the stator row were determined.

The anemometer signals were analyzed in a Fast Fourier Transform analyzer utilizing an ensemble averaging technique in which the analyzer was triggered by a once-per-revolution signal. This signal was produced by a magnetic pickup located on the rotor shaft and was recorded on the data tape. Four hundred samples were used for each ensemble average. The analysis time was selected to allow 52 points per blade gap thus ensuring good resolution of the blade wake defects. In the chosen time range of 4 milliseconds, the wakes from approximately half of the blades are displayed.

RESULTS AND DISCUSSION

The wake data presented are for the midspan and tip regions. They cover three axial distances behind the rotor. As was pointed out in the APPARATUS AND PROCEDURE section, the data at 1.23 chords were obtained with the stator located at 1.77 chords, whereas the remaining data were obtained within the plane of the stator leading edges. Data are shown for cases in which the fan stage was operated statically and with a tunnel velocity of 41 m/sec. In addition to the waveforms of both the streamwise and upwash velocity components, estimates of the peak to peak magnitude of the wake velocity and the wake width derived from the waveforms are presented. Finally the spatial harmonic content of the wake field is presented.

Midspan Region

Figures 4 through 7 show the signal enhanced waveforms of the rotor wakes in the midspan region (7.21 cm immersion) as a function of downstream distance from the rotor blades. The waveforms have been superimposed so that a direct comparison of shape with increased spacing can be made. The waveforms were overlaid such that the zero crossings on the ordinate scale for the majority of the waveforms would align.

Figures 4 and 5 show the effect of axial spacing on the streamwise and upwash components of the rotor wakes with static tunnel operations. The shapes are shown for seven consecutive rotor blades. Qualitatively, there is not much blade-to-blade variation at a given downstream location. It can be seen that the wake shapes at the closest spacing have a more complex structure than at the farther spacings. Although the radial component was not measured, it is possible that it was of high enough velocity at 0.54 rotor chords to contaminate the signals measured by the cross film, thus producing an irregular shape of the waveform. The wakes become smaller in amplitude, greater in width, and simpler in shape with increased distance from the rotor. At the 1.77 chord spacing the upwash component has almost disappeared.

The effect of forward velocity on the streamwise and upwash component wake shapes is seen in figures 6 and 7. With forward velocity, the wake shapes are qualitatively similar to those observed with static tunnel operation. The higher "spatial" harmonic content is considerably reduced in amplitude but still evident at the closest axial spacing. Forward velocity changes the turbulence characteristics of the flow entering the inlet due to the reduction in stream tube contraction ratio that occurs with flow no longer being drawn over the fan cowl from the aft direction. This causes a "cleanup" of the inflow and has a significant effect on the noise generated by a fan due to the rotor interaction with inflow disturbances (see refs. 12 and 13). The effects of freestream turbulence on rotor wake properties were systematically studied by Hah and Lakshminarayana (ref. 14). A large reduction in the inflow turbulence intensity resulted in a minimal change in the mean velocity defect.

The majority of the waveforms shown in figures 4 through 7 are asymmetric, but, as pointed out previously, are similar from blade to blade. There is no region between blades where a uniform mean flow exists as in the waveforms measured by Fessler and Hartmann at a downstream axial spacing of 0.8 chords.[15] This indicates that the wakes are already tending to merge at the near spacing of 0.54 rotor chords.

For noise and other purposes, one is interested in the decay characteristics of the wake as a function of downstream distance. In order to measure the change in velocity in the wake, a wake parameter, $\Delta V_w/V_{freestream}$ where ΔV_w is the peak-to-peak velocity in the wake, was defined. The effect of downstream distance on the absolute value of the wake parameter $\Delta V_w/V_{freestream}$ is shown in figure 8. The absolute values of the wake parameter for both the streamwise and upwash components decrease with increased distance. With the exception of the single data point observed with forward velocity at 0.54 chords, the data show little effect of forward velocity. Both the streamwise and upwash wakes decay at essentially the same rate. The streamwise wake defect magnitude is larger than the magnitude of the wake upwash by a nearly constant amount. The linear behavior of the data suggests that the wake shape as measured, midway between the stator vanes was not affected by the proximity of the vanes (recall that the data for the 1.23 chord spacing were obtained with the vanes at 1.77 chords whereas the data at the other two spacings were taken in the plane of the stator leading edges). The waveform in figure 7 corresponding to the deviant data point in figure 8 is considerable different from the other waveforms and it is unrepeatable from blade to blade showing two small velocity defects behind some blades but not behind others. The significance of this observation is unknown at present.

A second parameter used to describe the wake is the wake width. The wake width, as sketched in figure 9, is measured at the point where the velocity through the wake is half of its extreme value. The width is defined as the sum of the widths on the pressure and suction sides of the blade ($L_1 + L_2$) normalized by the blade spacing (S).

The effect of downstream distance on the rotor wake width is shown in figure 9. The width of the streamwise wake increases with downstream distance corresponding to the spreading of the wake. The upwash wake width also increases with downstream distance but appears to pass through a minimum at the intermediate distance. As in the case of the velocity defects, the wake widths show little effect of forward velocity except for the data point at 0.54 chords that has already been discussed in connection with its waveform and velocity defect magnitude.

At the farthest downstream location, the widths of the two wake components were equal. This result might have been anticipated: the wakes tend to merge with increasing distance approaching a sinusoidal shape. Given this simpler shape and that the two wake components are resolutions in the stator reference frame of the same wake, the two components could be equal.

Tip Region

Figures 10 through 13 show the signal enhanced waveforms in the near tip region. A probe immersion of 1.27 cm from the outer casing which was just outside the boundary layer was chosen. Figures 10 and 11 show the waveforms of the two velocity components measured with static tunnel operation. The complex waveforms of the streamwise component are characterized by two distinct narrow velocity defects at the 0.54 chord position. At further distances, the two velocity defects of the streamwise component (fig. 10) seem to form one large velocity defect. The upwash component shows two regions of increased velocity in each waveform corresponding to the defects in the streamwise component. Unlike the streamwise velocity, however, the two regions persist when the distance behind the rotor is in-

creased. Again, as for the midspan wake shapes, the tip wake shapes are remarkably similar from blade to blade.

The effect of forward velocity on the tip waveforms is shown in figures 12 and 13. These shapes of the waveforms are quite similar to those observed with static tunnel operation and show no clear distinguishing features not present in the static waveforms. However, the two defects in each streamwise waveform tend to persist at greater downstream distances than they do statically.

The tip region waveforms are very complex which reflects the real flow through the rotor blade row. In the tip, the simple wakes and potential flows are complicated by interactions with the casing boundary flow as well as a number of secondary flows, for example, tip clearance flows, passage vortex flows, a scraping vortex flow due to relative flow of the rotor blades, etc. Some of these secondary flows are discussed by Dittmar[1], Magliozzi, et al.[4], and Fessler, et al.[15]. A tip vortex can be generated because of the clearance between the blade and the outer wall which allows communication between the pressure and suction sides of the blade thus resulting in a secondary flow. It could also be generated by the relative motion of the blade scraping the wall boundary layer and rolling it into a vortex. Since the radial component of the velocity field behind the blade was not measured, it is not possible to determine from figures 10 through 13 which defect in the tip region can be attributed to a tip vortex. There does not appear to be a simple way to characterize the wake decay in the complex three-dimensional flow at the blade tips. As the waveforms show, there is not a single wake present to define the decay and further, there is no simple way to define wake width as in the case of the midspan wakes. As a further complication, if there is a vortex present at the tip, it is highly unlikely that it was tracked downstream in the present data, since the radial immersion of the probe was kept constant when the axial spacing was increased. Thus, the precise value of examining the variation of the tip wake with axial distance is not clear; however, as an indicator of what occurred with downstream distance, we have chosen to characterize the wake region by discussing the change in velocity on the pressure side and suction side of each waveform.

Considering the pressure side of the waveform first, the data in figure 14 show a linear decay rate of the wake parameter, $\Delta V_w/V_{freestream}$, that is considerably greater than for the midspan wakes (fig. 8). The wake parameter of the suction side shows the same decay rate as did the midspan wakes over the first two stations but then decays at about the same rate as the pressure side did. At the farthest position, the wake parameter of both components of both sides of each waveform reach nearly the same value. Interestingly, this value is about the same as that of the midspan wake at this distance. Figures 14(a) and (b) suggest that there are no significant effects of forward velocity in these data. Complete understanding of the complex tip region will require additional data and analysis.

Fourier Transforms of Signal Enhanced Waveforms

The signal enhanced waveforms were analyzed by Fast Fourier Transform methods to determine their harmonic content. Data from this analysis are more descriptive of the waveform than measures such as the wake defect and wake width, especially for the complicated wave shapes observed. In addition, in this form the data are probably more useful for analysis of the noise caused by the wakes passing across the stators. There is a direct

frequency correspondence between the harmonics of the wake and the harmonics of the sound field generated in the wake stator interaction.

Typical spectra of the signal enhanced wake velocities measured statically at the 0.54 chord station are shown in figure 15. Figure 15(a) compares the tip and midspan region of the streamwise component while figure 15(b) compares the upwash component. These spectra indicate high levels of the blade passage frequency and its second and fourth harmonics in the midspan region while the blade passage frequency and its second and third harmonic are predominant in the tip region. The next two figures utilize data from spectra such as those for the streamwise and upwash wake components, to examine the changes with downstream distance, to compare the midspan and tip regions and to examine the effect of forward velocity.

Midspan Spectra

Figures 16(a) and (b) show the effect of downstream distance on the harmonic content of the midspan streamwise and upwash wake components. At the closest position the dominant harmonics are the fundamental, second, and fourth. In fact, for the upwash component, the second and fourth harmonics were stronger than the fundamental accounting for the characteristics of that waveform. Proceeding downstream, the fundamental becomes dominant with a noticeable contribution of the second harmonic. The dominance of the fundamental corresponds to the wake shape becoming more sinusoidal with increasing downstream distance.

The effect of forward velocity is also shown and it can be seen to be a small effect in general. The effect is the most consistent at the closest spacing where several harmonics, notably the fourth and particulary in the upwash component, were reduced with forward velocity.

Tip Spectra

Figures 17(a) and (b) show the corresponding data for the tip region. Again the fourth harmonic was most affected by forward velocity, but in this case forward velocity increased it whereas for the midspan data it was reduced.

At the closest position, the first three harmonics all contribute to the statically measured wake. With forward velocity, the fourth harmonic described previously is also a contributor. The harmonics are all generally higher in the tip region than in the midspan region corresponding to the increased amplitude of the tip wakes. The other difference between the tip and midspan is the reduced contribution of the third harmonic in the midspan data.

As downstream distance increases the higher harmonics again decrease more rapidly than the fundamental and second harmonic corresponding to the reduction in wake shape complexity; however, in the near tip case the second harmonic persists and accounts for the more complex shape of the tip wake at the larger downstream distances.

There is not much to distinguish the upwash and streamwise components from each other in these data. Their harmonic content and its variation with downstream distance is quite similar.

SUMMARY OF RESULTS

An experiment was conducted to determine the effects of downstream distance on the mean wake properties behind a highly loaded fan rotor. The wake waveforms were measured and analyzed at both the midspan and near tip region. The majority of the waveforms are characterized by an asymmetric wake shape which remains similar from blade to blade.

In the midspan region, the waveforms of the wake are very irregular at the near spacing. This may be due to a contamination of the anemometry signal by the radial velocity component. Tunnel flow had a tendency to smooth the mean waveform through the wake but overall the effect of tunnel flow was minimal. As expected, the parametric study indicated that for the majority of conditions analyzed, the absolute value of the change in velocity in the wake decreased while the width increased with downstream distance.

In the near tip region, two distinct narrow regions of velocity change are present in each waveform at the near spacing. These regions remain distinct in the upwash component, but tend to merge in the streamwise component to form one large velocity defect. The rate of decay of the absolute value of the velocity in the region near the pressure side of the waveform is much faster at the close spacing than that near the suction side.

Spectral analysis indicates that the fundamental, second, and third harmonics of the blade passing frequency dominate the tip region while the fundamental, second, and fourth harmonics dominate the midspan region.

Although only two components of velocity were measured in the present experiment, the data presented in this paper has provided insight into the complex nature of the velocity components of the rotor wake in the stationary reference frame of a highly loaded rotor. It is hoped that the analysis of the harmonic content of the rotor wake waveforms will lead to an understanding of the complex nature of the fan noise generated by the velocity field surrounding the stator vanes.

REFERENCES

1. Dittmar, J. H., "Interaction of Rotor Tip Flow Irregularities with Stator Vanes as a Noise Source," NASA TM-73706, 1977.
2. Hirsch, C. H. and Kool, P., "Measurement of the Three-Dimensional Flow Behind Axial Compressor State," ASME Paper 76-GT-18, Mar. 1976.
3. Evans, R. L., "Turbulence and Unsteady Measurements Downstream of a Moving Blade Row," ASME Paper 74-GT-73, Mar. 1974.
4. Magliozzi, B., Hanson, D. B., Johnson, B. V., and Metzger, F. B., "Noise and Wake Structure Measurements in a Subsonic Tip Speed Fan," NASA CR-2323, 1973.
5. Bennett, J. C., "Measurements of Periodic Flow in Rotating Machinery," AIAA Paper 77-713, June 1977.
6. Reynolds, B. and Lakshminarayana, B., "Characteristics of Lightly Loaded Fan Rotor Blade Wakes," NASA CR-3188, 1979.
7. Ravindranath, A. and Lakshminarayana, B., "Three Dimensional Mean Flow and Turbulence Characteristics of the Near Wake of a Compressor Rotor Blade," Pennsylvania State University, University Park, PA, PSU-TURBO-R-80-4, June 1980. (NASA CR-159518.)
8. Yuska, J. A., Diedrich, J. H., and Clough, N., "Lewis 9- by 15-Foot V/STOL Wind Tunnel," NASA TM X-2305, 1971.

9. Rentz, P. E., "Softwall Acoustical Characteristics and Measurement Capabilities of the NASA Lewis 9x15 Foot Low Speed Wind Tunnel," Bolt, Beranek, and Newman, Inc., Canoga Park, CA, BBN-3176, June 1976. (NASA CR-135026.)
10. Lewis, G. W., Jr. and Tysl, E. R., "Overall and Blade-Element Performance of the 1.20-Pressure-Ratio Fan Stage at Design Blade Setting Angle," NASA TM X-3101, 1974.
11. Abbott, J. M., Diedrich, J. H., and Williams, R. C., "Low-Speed Aerodynamic Performance of 50.8-Centimeter-Diameter Noise-Suppressing Inlets for the Quiet, Clean, Short-Haul Experimental Engine (QCSEE)," NASA TP 1178, 1978.
12. Heidmann, M. F. and Dietrich, D. A., "Simulation of Flight-Type Engine Fan Noise in the NASA Lewis 9x15 Anechoic Wind Tunnel," NASA TM X-73540, 1976.
13. Shaw, L. M., Woodward, R. P., Glaser, F. W., and Dastoli, B. I., "Inlet Turbulence and Fan Noise Measured in an Anechoic Wind Tunnel and Statically with an Inlet Flow Control Devise," NASA TM-73723, 1977.
14. Hah, C. and Lakshminarayana, B., "Free Stream Turbulence Effects on the Development of Rotor Wake," AIAA Paper 80-1431, July 1980.
15. Fessler, T. E. and Hartmann, M. J., "Preliminary Survey of Compressor Rotor-Blade Wakes and Other Flow Phenomena with a Hot-Wire Anemometer," NACA RM E56A13, 1956.

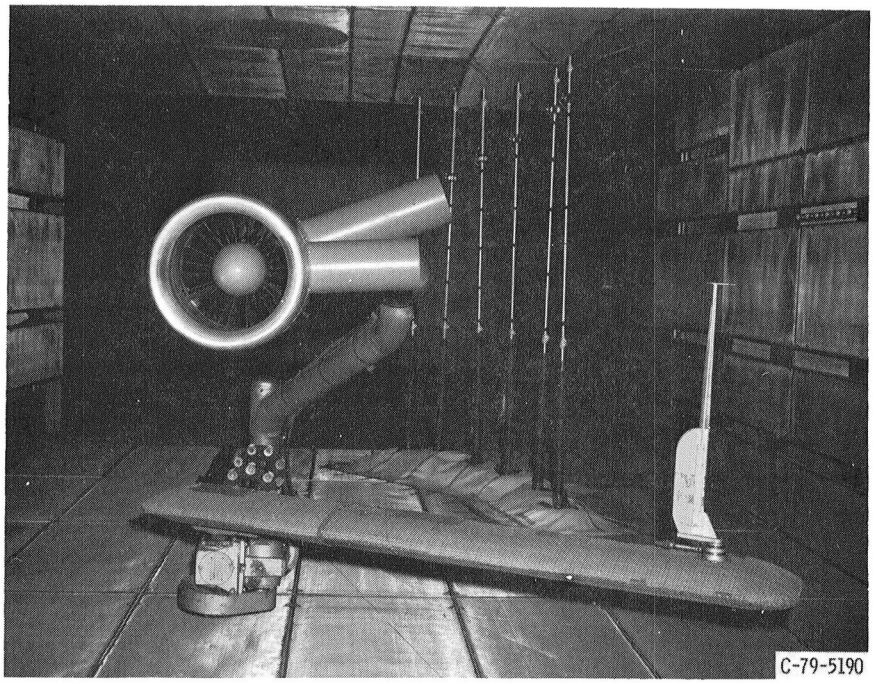

Figure 1. - Upstream view of fan simulator in anechoic tunnel.

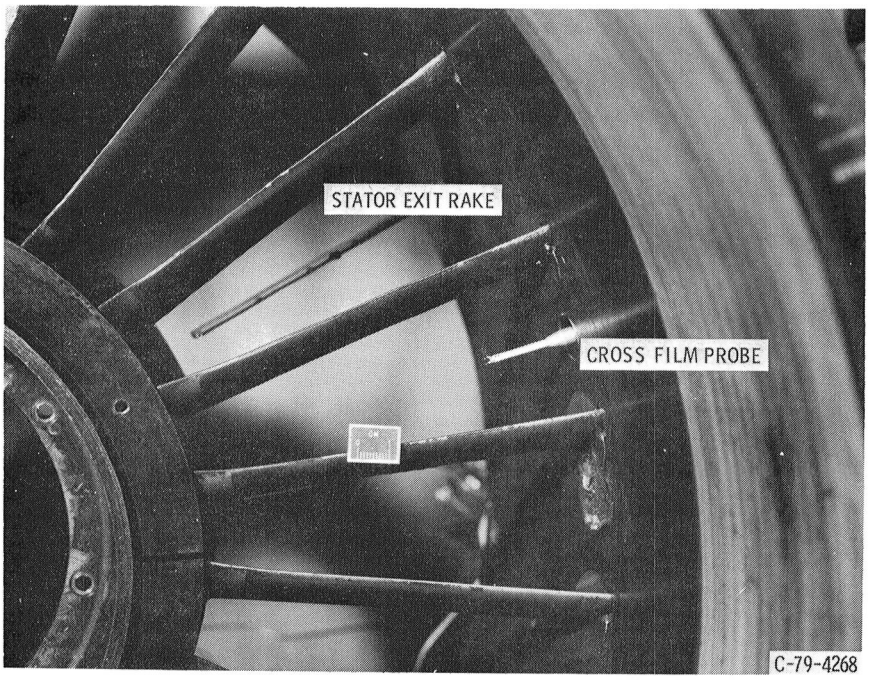

Figure 2. - Position of cross film relative to stator vanes.

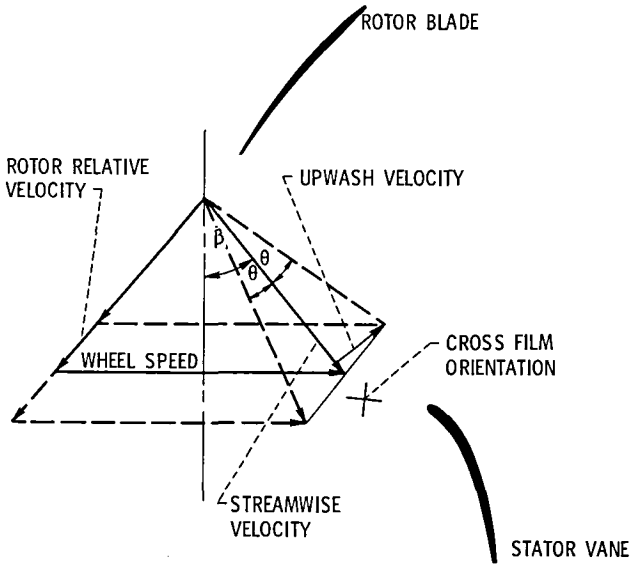

Figure 3. - Schematic of cross film orientation (β = probe set angle, θ = fluctuating angle about β).

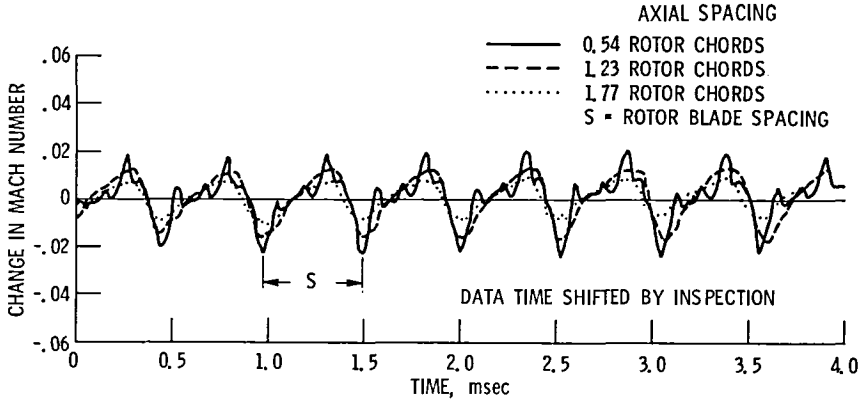

Figure 4. - Midspan signal enhanced waveforms for the streamwise component, 96% design rpm, 7.21 cm immersion (53% of span from tip). Static tunnel operation (U = 0).

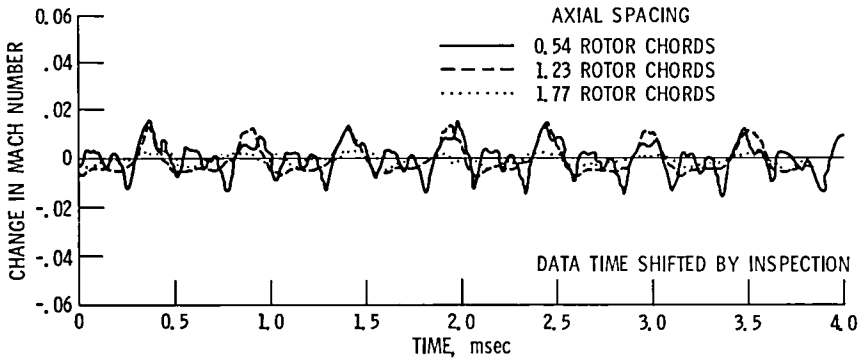

Figure 5. - Midspan signal enhanced wave forms of the upwash component, 96% design rpm, 7.21 cm immersion (53% of span from tip). Static tunnel operation (U = 0).

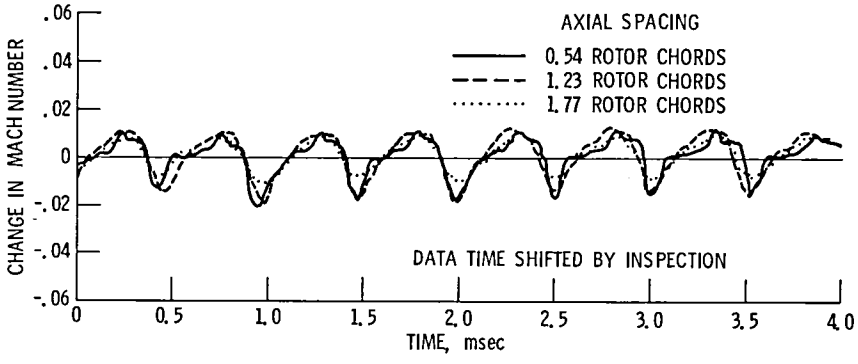

Figure 6. - Midspan signal enhanced waveforms of the streamwise component, 96% of design rpm, 7.21 cm immersion (53% of span from tip), forward velocity condition (U = 41 m/sec).

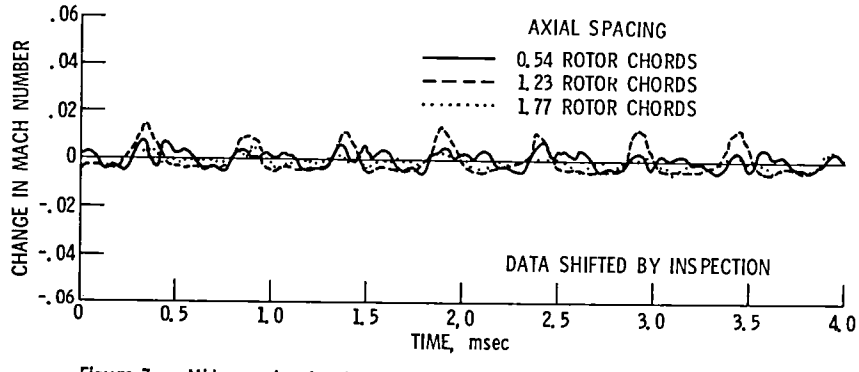

Figure 7. - Midspan signal enhanced waveforms of the upwash component, 96% of design in rpm, 7.21 cm immersion (53% of span from tip), forward velocity condition (U = 41 m/sec).

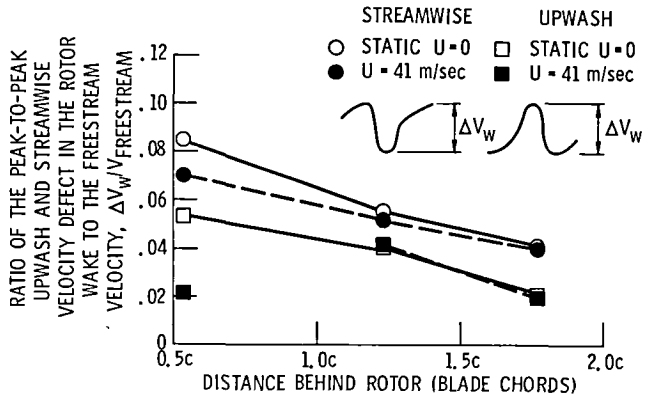

Figure 8. - Effect of downstream distance and forward velocity of the change in the upwash and streamwise velocity components in the wake in the midspan region.

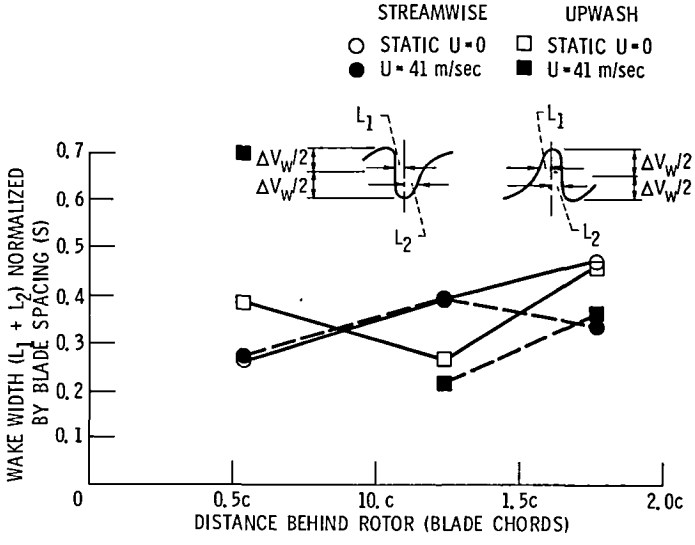

Figure 9. - Effect of distance behind rotor blades and forward velocity on the width of the rotor wake in the midspan region.

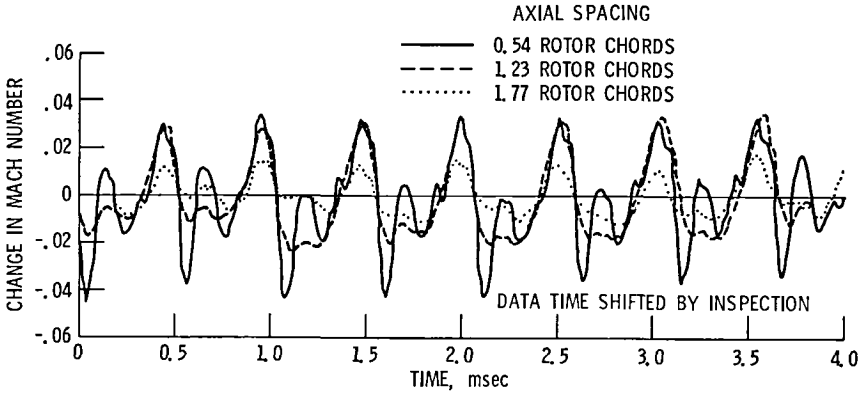

Figure 10. - Tip region signal enhanced waveforms of the streamwise component, 96% of design rpm, 1.27 cm immersion (9.0% of span from tip), static tunnel operation (U = 0).

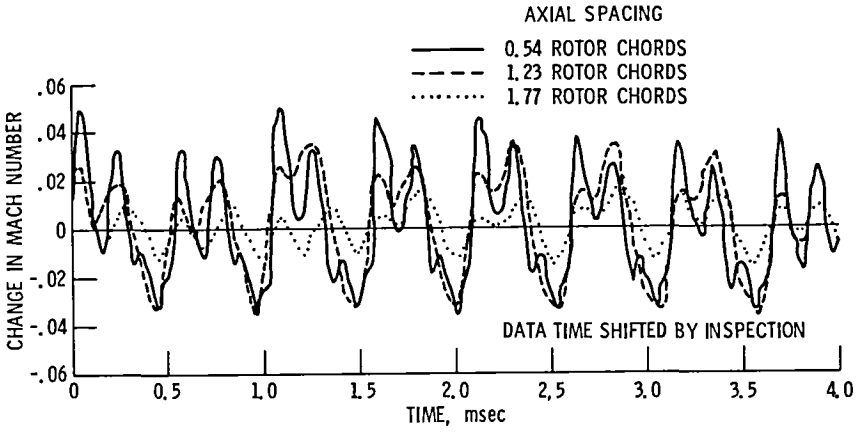

Figure 11. - Tip region signal enhanced waveforms of the upwash component, 96% of design rpm, 1.27 cm immersion, (9.0% of span from tip) static tunnel operation (U = 0).

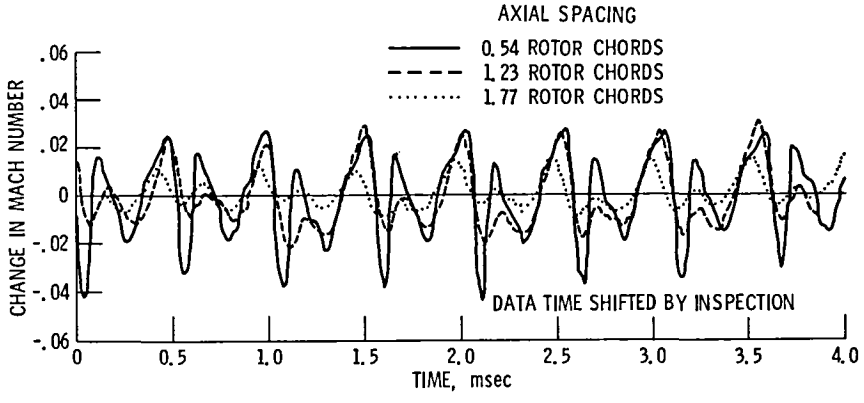

Figure 12. - Tip region signal enhanced waveforms of the streamwise component, 96% of design rpm, 1.27 cm immersion (9.0% of span from tip) forward velocity condition (U = 41 m/sec).

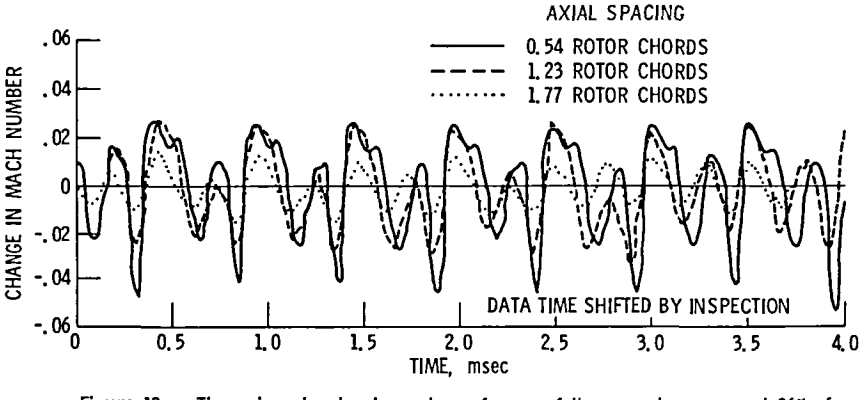

Figure 13. - Tip region signal enhanced waveforms, of the upwash component 96% of design rpm, 1.27 cm immersion (9.0% of span from tip), forward velocity condition (U = 41 m/sec).

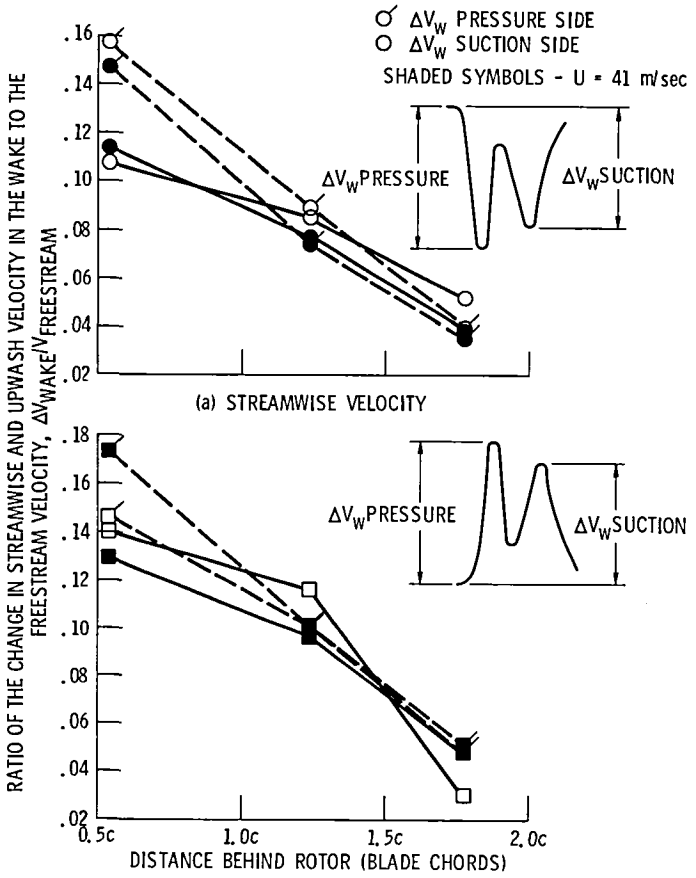

Figure 14. - Effect of downstream distance and tunnel flow on the change in velocity in the wake in the near tip region.

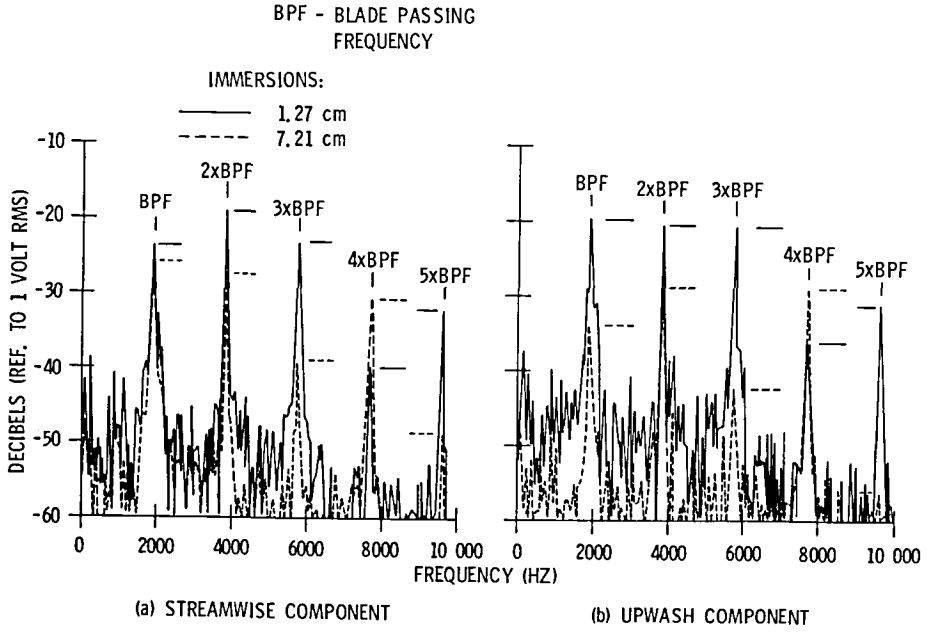

Figure 15. - Spectra of signal enhanced wake velocities, 96% design rpm, static tunnel operation (U = 0), 0.54 chord axial spacing.

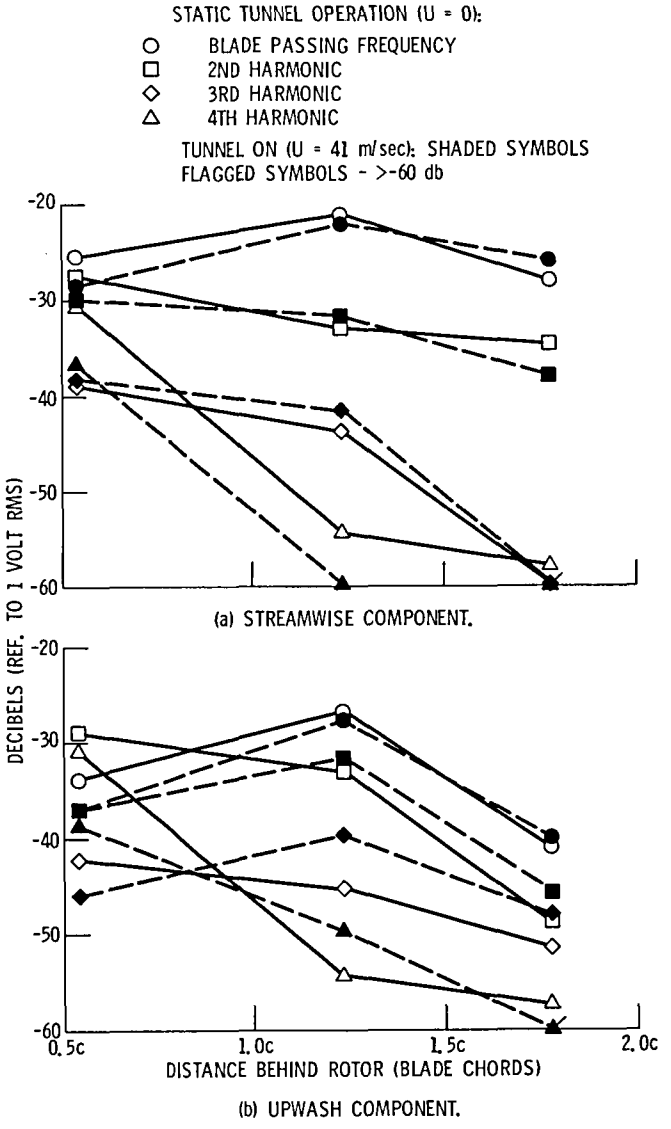

Figure 16. - Harmonic levels from signal enhanced spectra, 96% of design rpm, 7.21 cm immersion, 53% of span from tip.

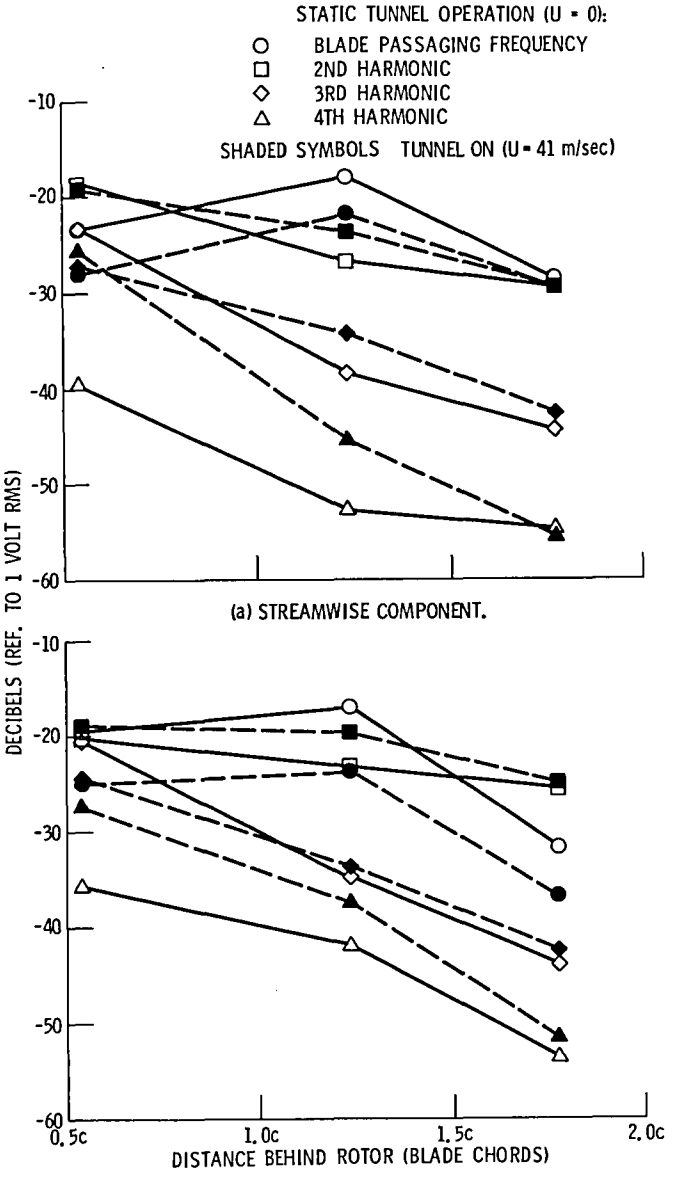

Figure 17. - Harmonic levels from signal enhanced spectra, 96% of design rpm, 1.27 cm immersion (9.0% of span from tip).

1. Report No. NASA TM-81657	2. Government Accession No.	3. Recipient's Catalog No.
4. Title and Subtitle MEAN ROTOR WAKE CHARACTERISTICS OF AN AERODYNAMICALLY LOADED 0.5 M DIAMETER FAN		5. Report Date 6. Performing Organization Code 505-32-02
7. Author(s) L. M. Shaw and F. W. Glaser		8. Performing Organization Report No. E-674 10. Work Unit No.
9. Performing Organization Name and Address National Aeronautics and Space Administration Lewis Research Center Cleveland, Ohio 44135		11. Contract or Grant No. 13. Type of Report and Period Covered Technical Memorandum
12. Sponsoring Agency Name and Address National Aeronautics and Space Administration Washington, D.C. 20546		14. Sponsoring Agency Code

15. Supplementary Notes

Prepared for the Nineteenth Aerospace Sciences Meeting sponsored by the American Institute of Aeronautics and Astronautics, St. Louis, Missouri, January 12-15, 1981.

16. Abstract

Mean rotor wake properties at several downstream distances behind the rotor of a loaded 1.2 pressure ratio fan were measured with a cross film anemometer in an anechoic wind tunnel. Mean wake characteristics in the midspan and near tip region were determined utilizing an ensemble averaging technique. The upwash and streamwise components of the velocity behind the rotor indicate a complex structure superimposed on the major velocity defects at a downstream spacing of 0.5 rotor chords. Spectral analysis indicates high levels of the second and fourth harmonics of the blade passage frequency in the midspan region while the blade passage frequency and its second and third harmonic are predominant in the tip region.

17. Key Words (Suggested by Author(s))	18. Distribution Statement
Turbomachinery Rotor wakes	Unclassified - unlimited STAR Category 07

19. Security Classif. (of this report)	20. Security Classif. (of this page)	21. No. of Pages	22. Price*
Unclassified	Unclassified		

* For sale by the National Technical Information Service, Springfield, Virginia 22161

National Aeronautics and Space Administration

Washington, D.C.
20546

Official Business
Penalty for Private Use, $300

SPECIAL FOURTH CLASS MAIL
BOOK

Postage and Fees Paid
National Aeronautics and
Space Administration
NASA-451

NASA

POSTMASTER: If Undeliverable (Section 158 Postal Manual) Do Not Return